PNAS
www.pnas.org

Supporting information for

Mmp-induced fat body cell dissociation promotes pupal development and attenuates pupal diapause by activating lipid metabolism

Qiangqiang Jia and Sheng Li

Corresponding author: Sheng Li

Email: lisheng@scnu.edu.cn

This PDF file includes:

SI Materials and Methods

SI References

Figure S1 to S10

Table S1

Legends for Datasets S1 to S2

Other supplementary materials for this manuscript include the following:

Datasets S1 and S2

SI Materials and Methods

Insect rearing and chemicals. The colony of *H. armigera* was provided by Dr. Yidong Wu in Nanjing Agricultural University and maintained on an artificial diet in our laboratory (1). To produce the diapause pupae used in this study, larvae were reared during the L: D= 10: 14 photoperiod at 20 ℃. The nondiapause pupae were produced by rearing larvae during the L: D= 14: 10 photoperiod at 20 ℃. The incidence of pupal diapause was determined by the eyespots that did not move 10-15 days after pupation. The colony of *S. frugiperda* was provided by Dr. Kongming Wu in Institute of Plant Protection, Chinese Academy of Agricultural Science and maintained on an artificial diet in our laboratory during the L: D= 14: 10 photoperiod at 28 ℃ (2). The *D. melanogaster* stocks were reared on standard cornmeal-molasses medium during the L: D= 14: 10 photoperiod at 25 ℃.

The cathepsin L specific inhibitor CAA0225 (Catalog number: 219502, Merck), broad spectrum MMPs inhibitor GM6001 (Catalog number: S7157, Selleck), and lipases inhibitor Orlistat (Catalog number: O4139, Merck) was dissolved in DMSO as a concentration of 10 mM. Three microliters of DMSO was injected as a control on the day of pupation, and 3 μL of inhibitors was injected as a treatment.

Measurement of enzymatic activity. Pupal brain were dissected in PBS and stored at -80 ℃ until use. Brain COX activity was measured using the Cytochrome c Oxidase Assay Kit (Catalog number: CYTOCOX1, Merck) according to the manufacturer's instructions. Abdominal peripheral fat body was collected into 1.5 ml eppendorf tubes. Then fat body Cathepsin L activity, Mmps activity, and Lipases activity were measured by using the Cathepsin L Activity Assay kit (Fluorometric) (Catalog number: ab65306, Abcam), the total MMP Fluorescent Assay Kit (Catalog number: GMS50048.2, Genmed Scientifics, Shanghai, China) and the Lipase Assay Kit III (Fluorometic) (Catalog number: ab118969, Abcam) according to the manufacturer's instructions, respectively.

Measurement of nutrients in the hemolymph and fat body. Hemolymph was collected and pooled from 10 pupae of corresponding time points with 1.5 ml eppendorf tubes containing

phenylthiourea, then centrifuged at 1000× g, 4 ℃ for 5 min to remove hemocytes. The supernatants were incubated with different analysis reagents.

DAG and FFA in the hemolymph supernatant was measured using Triglyceride assay kit (Catalog number: A110-1-1) and Free Fatty Acids assay kit (Catalog number: A042-1-1) (Nanjing Jiancheng Bioengineering Institue, China), respectively. Hemolymph trehalose, glucose, and amino acids were measured using Trehalose Assay Kit (Catalog number: K-TREH, Megazyme, USA), Glucose Content Assay kit (Catalog number: BC2505), and Amino Acid Content Assay Kit (Catalog number: BC1575) (Solarbio Life Sciences, Beijing, China), respectively. Total proteins in the hemolymph were measured by BCA Protein Assay kit (Catalog number: 20201ES76, Yeasen, Shanghai, China). Data was normalized to hemolymph volume.

The fat body (about 0.1 g) was homogenized by using 0.5 ml PBST (PBS+0.1% Triton X-100) buffer, then centrifuged the samples at 10000× g, 4 ℃ for 10 min to remove debris. The supernatant was assayed directly by Glycogen Assay Kit (Catalog number: MET-5022, Cell Biolabs, Inc). The protein concentration in the supernatant was measured by BCA Protein Assay Kit. The glycogen content data was normalized to protein content.

Cell culture and tranfection. HaEpi cells were derived from the 5th instar *H. armigera* larval epidermis and were generously provided by Dr. Xiaofan Zhao in Shandong University (3). Cells were cultured at SIM SF Expression Medium (Catalog number: MSF1, Sino Biological, Beijing, China) supplemented with 5% fetal bovine serum (Catalog number: SH30088.03, HyClone). cDNAs of *GFP*, *Har-CatL*, *Har-Mmp1*, *Har-Mmp2*, *Har-Mmp3*, and *Har-Timp* were cloned into the pIZ/V5-His vector. Har-CatL was fused with Myc epitope tag and other proteins were fused with V5 epitope tag on the C-terminal. The constructs were transfected or co-transfected into HaEpi cells using Effectene Transfection Reagent (Catalog number: 301427, QIAGEN) according to the manufacturer's instructions.

RNAi of *Har-CatL* in *H. armigera*. Using pIZ-GFP-V5-His and pIZ-Har-CatL-Myc as PCR templates, the primers annealing to T7 promoter sequence (the forward primer and reverse primer are listed in Table S1) were used for PCR amplification of the dsRNA templates. The dsRNA was synthesized using T7 RiboMAX Express RNAi Kit (Catalog number: P1700, Promega) according

to the manufacturer's instructions. The dsRNAs were injected into the abdomen of *H. armigera* by 15 μg per pupae at day 0 after pupation. GFP dsRNA was injected as a control.

Expression and purification of recombinant Har-Mmp2 in *E. coli*. The coding sequence of active form of Har-Mmp2 (without transmembrane domain) was amplified by PCR and cloned into the pET28a plasmid, with a C-terminal 6 × His tag for purification. The expression, purification and refolding of rHar-Mmp2 was performed as previously described (4). GFP protein was used as control and purified by using the same method.

Fly strains and genetics. All fly strains were grown at 25 ℃on standard cornmeal/molasses/agar medium. Synchronization was performed at white prepupa (WPP) stage. *Lsp2-Gal4* or *Gal80^{ts}; Lsp2-Gal4* was used to drive fat body specifically gene knockdown or overexpression. *UAS-Dm-CatL-RNAi* (v13959) was obtained from the Vienna *Drosophila* RNAi Center, *UAS-Dm-CatL-3×HA* (F001040) was obtained from Fly ORF.

The cDNAs of *Har-CatL*, *Har-Mmp1*, *Har-Mmp2*, and *Har-Mmp3* were cloned into the pUAST vector. The four UAS constructs were used to produce transgenic flies using P-element-mediated germline transformation by Core Facility of *Drosophila* Resource and Technology, Center for Excellence in Molecular Cell Science (CEMCS), Chinese Academy of Science (CAS).

Generation of *Har-Mmp2* and *Har-Timp* mutants by CRISPR/Cas9. A PCR-based approach was used to prepare sgRNA according to the manufacturer's instruction (Catalog number: AM1333, MEGAscript® Kit, Thermo Fisher Scientific). Primer sequences used were detailed in supplementary Table S1. The collection and preparation of eggs were carried out as reported previously (1). A mix of sgRNA1 (200 ng/μl), sgRNA2 (200 ng/μl), and Cas9 protein (200 ng/μl, Catalog number: A36498, TrueCut™ Cas9 Protein v2, Thermo Fisher Scientific) was injected into embryos using a micro-injector (FemtoJet®, Germany). The injected eggs were incubated at 25℃ for 3-4 days until hatching. The hatched animals were G0 individuals. The adults of G0 were single-pair mated each other to produce G1 individuals. Genomic DNA was extracted from the larvae-sloughs of G1 individuals for genotyping by sequencing. G2 individuals come from

inbreeding of G1 were genotyped by PCR and used for experiments. The detailed procedures were reported by Wang et al (5).

Co-immunoprecipitation (Co-IP) analysis. HzAm1 cells transfected with GFP or recombinant plasmids were lysed in NP-40 lysis buffer (Catalog number: P0013F, Beyotime Biotechnology). The lysates were incubated at 4 ℃ for 30 min and then centrifuged for 20 min at 12000× g, 4 ℃. The protein was incubated overnight with primary antibodies and 30 μl protein A/G agarose suspensions (Catalog number: 20421, Thermo Fisher Scientific) and analyzed by Western blot.

qPCR and Western blot analysis. Total RNA was extracted from *H. armigera* abdominal peripheral fat body by using Trizol reagent (Catalog number: AG21101, Accurate Biotechnology, Hunan, China). After quantification, 2 μg of total RNA was reverse transcribed at 42 for 1 h using the Reverse Transcriptase M-MLV (Catalog number: 2641B, Takara, Japan). qPCR was performed using Hieff® qPCR SYBR Green Master Mix (Low Rox Plus) (Catalog number: 11202ES03, Yeasen) and the Applied Biosystems™ QuantStudio™ 6 Flex Real-Time PCR System. All qPCR primers used in this study are listed in supplementary Table S1.

Total proteins were extracted from the fat body or brain by using RIPA lysis buffer (P0013B, Beyotime Biotechnology), then were quantified using a BCA Protein Assay kit (Yeasen). The rabbit polyclonal antibodies were generated by immunization of rabbit with epitope DDVRHYAYEGDGNTS (E-cadherin), KLWDGYSLLYIDGNEKAHNQDLG (Collagen IV α1), GQDLGASGSCMRKFSTMPYMFC (Collagen IV α2), GQDLGASGSCMRKFSTMPYMFC (Har-Timp) by ChinaPeptides (Shanghai, China). The *Drosophila* Mmp2 rabbit polyclonal antibody was used to detect Har-Mmp2 (6). The *S. frugiperda* CatL mouse monoclonal antibody was used to detect Har-CatL (Catalog number: MAB22591-SP, Bio-Techne). Antibodies against p-InR (Catalog number: 3024, detect Tyr1150/1151 phosphorylated InR in human and Tyr1220/1221 phosophorylated InR in *H. armigera*) were purchased from Cell Signaling Technology; p-FoxO (Catalog number: ab131339, detect Serine256 phosphorylated FoxO in human and Serine191 phosphorylated FoxO in *H. armigera*) was purchased from Abcam. *H. armigera* FoxO antibody was generously provided by Dr. Wei-Hua Xu in Sun Yat-Sen University. Myc epitope tag antibody (Catalog number: 2276S) and V5 epitope tag antibody (Catalog number:

13202S) were purchased from Cell Signaling Technology. All primary antibodies were diluted to 1/1000, and secondary antibodies were diluted to 1/5000.

Histological sections and hematoxylin-eosin staining. The abdominal fat body of corresponding time points was fixed in 4% formaldehyde at 4 ℃ overnight, then histological sections and hematoxylin-eosin (H&E) staining were performed as previously described (7).

Staining and microscopy. Fat body tissues were dissected from pupae of corresponding time points. To visualize lipid droplets, we stained the fixed tissues with BODIPY 493/503 (Catalog number: 790389-500MG, Merck). BODIPY 493/503 was dissolved in ethanol at 1 mg/ml, then diluted at 1:1000 in PBS and applied to tissue samples. The resulting fluorescence signals were examined under a confocal microscope Olympus FV3000.

Hemolymph lipidomics analysis. Hemolymph samples were mixed with triple volume of chloroform/methanol (2:1, v/v) at 4 ℃. Lipids were extracted on ice for 3 h, centrifuged at 8000 × g for 20 min at 4 ℃, and the resultant supernatant was concentrated to dryness under vacuum. The lipids were then dissolved in isopropanol (200 μL) and stored at -80 ℃ for subsequent analysis. The final samples are analyzed by LC-MS.

LC conditions: ACQUITY UPLC® BEH C18 1.7 μm (2.1 × 100 mm) chromatographic column was used for gradient elution. The automatic sampler temperature was set at 8 ℃, the flow rate was 0.25 mL/min, the column temperature was 50 ℃, the injection volume was 2 μL. The mobile phase was acetonitrile: water=60:40 (0.1 formic acid+10 mM ammonium formate) (solvent C) and isopropanol: acetonitrile=90: 10 (0.1% formic acid+10 mM ammonium formate) (solvent D). An increasing linear gradient of solvent D (v/v) was used.

MS conditions: electrospray ion source (ESI), positive and negative ion ionization mode, posive ion spray voltage of 3.50 kV, negative ion spray voltage of -2.50 kV, sheath gas of 30 Arb, auxiliary gas of 10 Arb. The capillary temperature was 325 ℃, and the scanning range was 150~2000 with a resolution of 35000. HCD was used for secondary cracking with a collision voltage of 30 eV, and the unnecessary MS/MS information was removed by dynamic elimination. Lipid peaks were analyzed and identified by using LipidSearch software. The peak intensity was

normalized based on quality controls (QCs). These QCs are pooled biological samples containing all the characteristics of the hemolymph samples under investigation. Differential abundant lipids were identified by VIP $\geqslant 1$ and p value $\leqslant 0.05$. The unsupervised clustering analysis was performed by using the OmicShare tools, a free online platform for data analysis (https://www.omicshare.com/tools).

Transcriptomic analysis. For fat body transcriptomic analysis, total RNA was extracted from the fat body of related genotypes of related time points by using Trizol reagent. RNA-sequencing libraries were prepared with the IlluminaTruSeq Stranded Total RNA Library Preparation Kit, and were sequenced on an Illumina HiSeq 4000 platform by Shanghai Personalbio Technology Co., Ltd. Four biological replicates were performed. Sequencing reads were aligned with Swissprot, eggNOG, GI, NR, and KEGG databases. Unigene abundance was measured by FPKM values and used for subsequent annotation and differential gene expression analysis. HTSeq was used to compare the Read Count value of each gene, and FPKM was used to standardize the expression level, while DESeq software was used for screening differentially expressed genes.

PCA analysis was performed using the OmicShare tools, and then PCA plots (Fig. 5C and 5D) were drawn by ChiPlot (https://www.chiplot.online/). For testing significance of gene overlaps (Fig. 5*C'* and 5*D'*), gene lists were ranked according to the product of the absolute log-fold-change multiplied by the log-converted P-value and then comparing the lists using the OrderedList Package (8-10). Scatterplots for showing the correlation between changes in gene expression (Fig. 5*C''* and *D''*) were drawn by ChiPlot (https://www.chiplot.online/).

Statistics. The experimental data were analyzed using Student's t-test and ANOVA by GraphPad Prism software v8.02 (San Diego, USA). For the t-test: *, $p<0.05$; **, $p<0.01$; ***, $p<0.001$. ANOVA: bars labeled with different lowercase letters are significantly different ($p<0.05$). Difference in rate of eyespot movement was determined using Kolmogorov-Smirnov test (11). Throughout the study, the values represent the mean $\pm$ standard deviation of 3 or more independent experiments.

SI References

1. J. Wang et al., Functional validation of cadherin as a receptor of Bt toxin Cry1Ac in *Helicoverpa armigera* utilizing the CRISPR/Cas9 system. *Insect Biochem. Mol. Biol.* **76**,11-17 (2016).
2. S. Ge et al., Potential trade-offs between reproduction and migratory flight in *Spodoptera frugiperda*. *J Insect Physiol.* **132**, 104248 (2021).
3. J. Pan et al., Insulin and 20-hydroxyecdysone oppose each other in the regulation of phosphoinositide-dependent kinase-1 expression during insect pupation. *J. Biol. Chem.* **293**, 18613-18623 (2018).
4. D. Wen, Z. Chen , Z. Zhang, Q. Jia. The expression, purification, and substrate analysis of matrix metalloproteinases in *Drosophila melanogaster*. *Protein Expr. Purif.* **171**, 105629 (2020).
5. J. Wang, H. Ma, Y. Zuo, Y. Yang, Y. Wu. CRISPR-mediated gene knockout reveals nicotinic acetylcholine receptor (nAChR) subunit α6 as a target of spinosyns in *Helicoverpa armigera*. *Pest Manag. Sci*. **76**, 2925-2931 (2020).
6. Q. Jia, Y. Liu, H. Liu, S. Li. Mmp1 and Mmp2 cooperatively induce *Drosophila* fat body cell dissociation with distinct roles. *Sci. Rep.* **4**, 7535 (2014).
7. X. Chen , L. Yang, R. Huang, S. Li, Q. Jia. Matrix metalloproteinases are involved in eclosion and wing expansion in the American cockroach, *Periplaneta americana*. *Insect Biochem. Mol. Biol.* **131**, 103551 (2021).
8. C. Lottaz, X. Yang, S. Scheid, R. Spang. OrderedList--a bioconductor package for detecting similarity in ordered gene lists. *Bioinformatics* **22**, 2315-2316 (2006).
9. J. Gospocic et al., The neuropeptide Corazonin controls social behavior and caste identity in ants. *Cell* **170**, 748-759 (2017).
10. J. Gospocic et al., Kr-h1 maintains distinct caste-specific neurotranscriptomes in response to socially regulated hormones. *Cell* 184, 5807-5823 (2021).
11. T. Nishimura. Feedforward regulation of glucose metabolism by steroid hormones drives a developmental transition in *Drosophila*. *Curr. Biol.* **30**, 3624-3632 (2020).

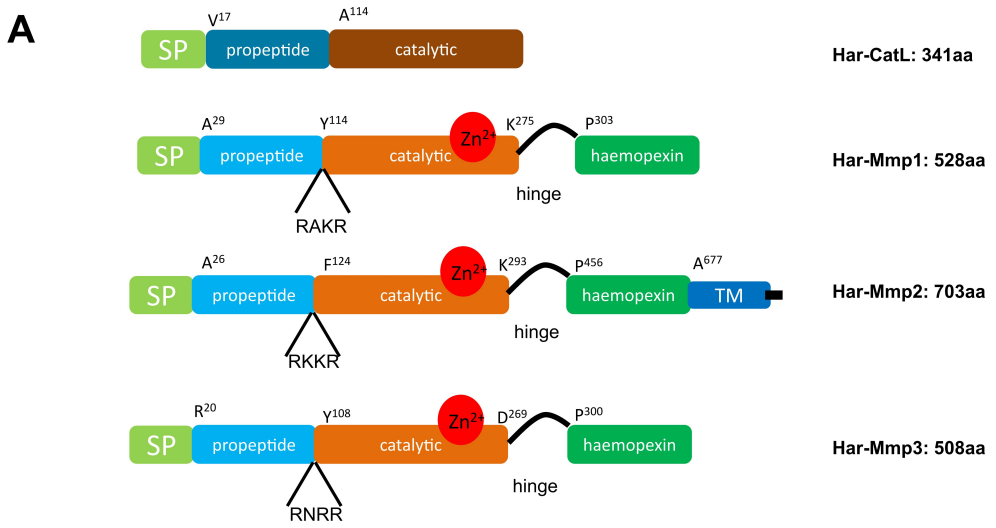
A
SP
propeptide
catalytic
V17
A114
Har-CatL: 341aa
A29
Y114
Zn2+
K275
P303
haemopexin
hinge
RAKR
Har-Mmp1: 528aa
A26
F124
K293
P456
A677
TM
RKKR
Har-Mmp2: 703aa
R20
Y108
D269
P300
RNRR
Har-Mmp3: 508aa

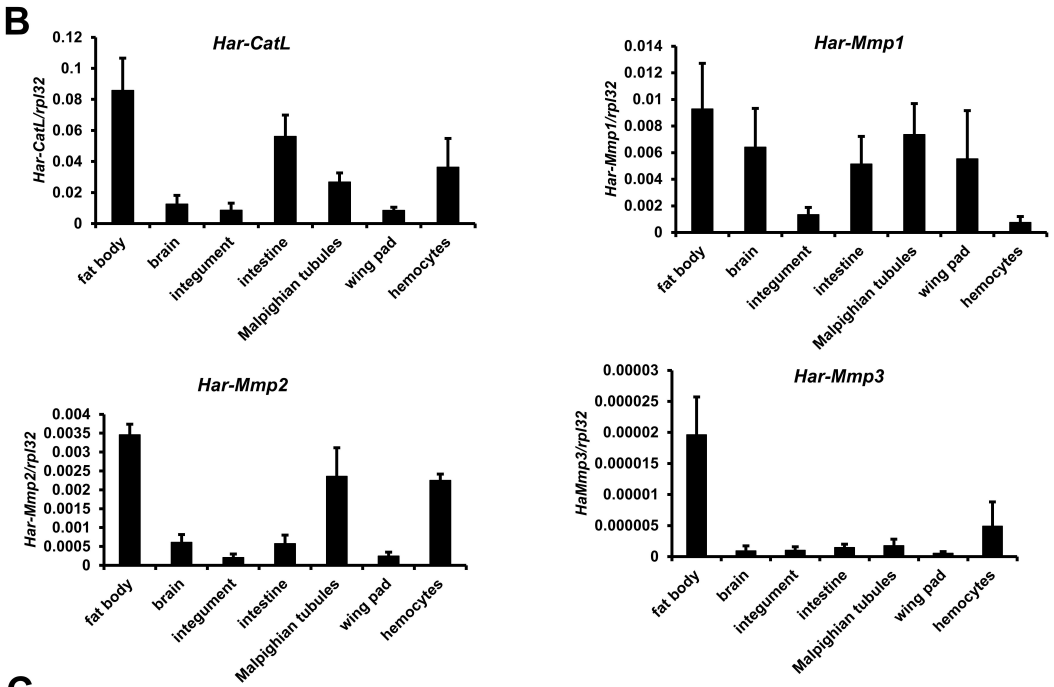
B
Har-CatL
Har-CatL/rpl32
Har-Mmp1
Har-Mmp1/rpl32
Har-Mmp2
Har-Mmp2/rpl32
Har-Mmp3
HaMmp3/rpl32
fat body
brain
integument
intestine
Malpighian tubules
wing pad
hemocytes

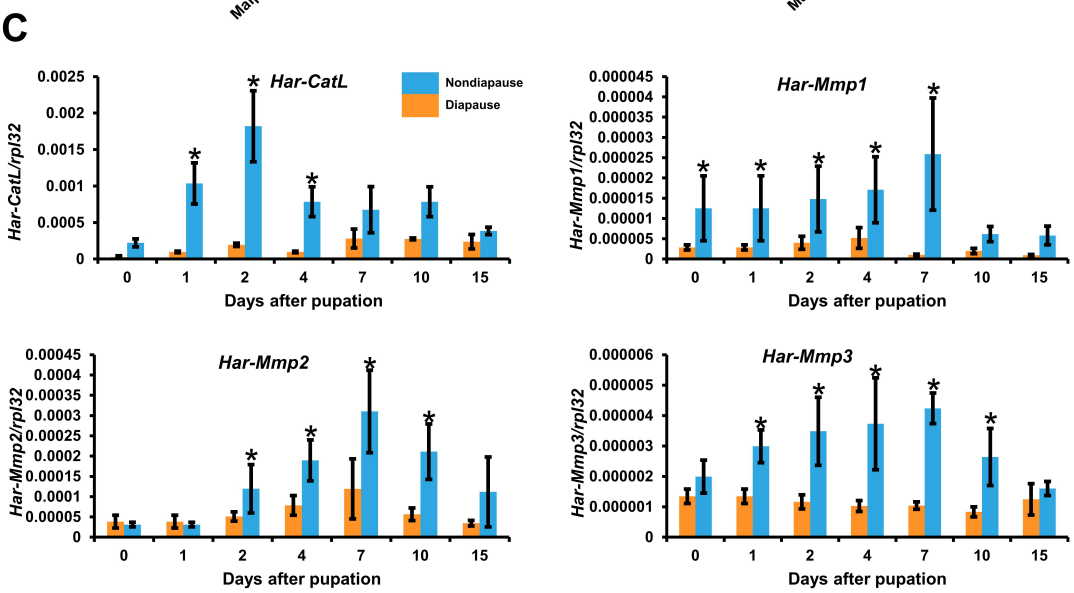
C
Har-CatL
Nondiapause
Diapause
Har-CatL/rpl32
Har-Mmp1
Har-Mmp1/rpl32
Har-Mmp2
Har-Mmp2/rpl32
Har-Mmp3
Har-Mmp3/rpl32
Days after pupation

Fig. S1. Structures and expression patterns of Har-CatL and Har-Mmps.

(*A*) Map of the key domain organizations in one Har-CatL and three Har-Mmps.

(*B*) Tissue distribution of *Har-CatL* and *Har-Mmps* in the nondiapause pupae 4 days after pupation.

(*C*) Developmental profiles of *Har-CatL* and *Har-Mmp* mRNA expression levels in the fat body in nondiapause pupae and diapause pupae.

Bars represent the mean ± SEM. Significant differences were calculated using Student's t test (*, $p<0.05$) according to three biological replicates.

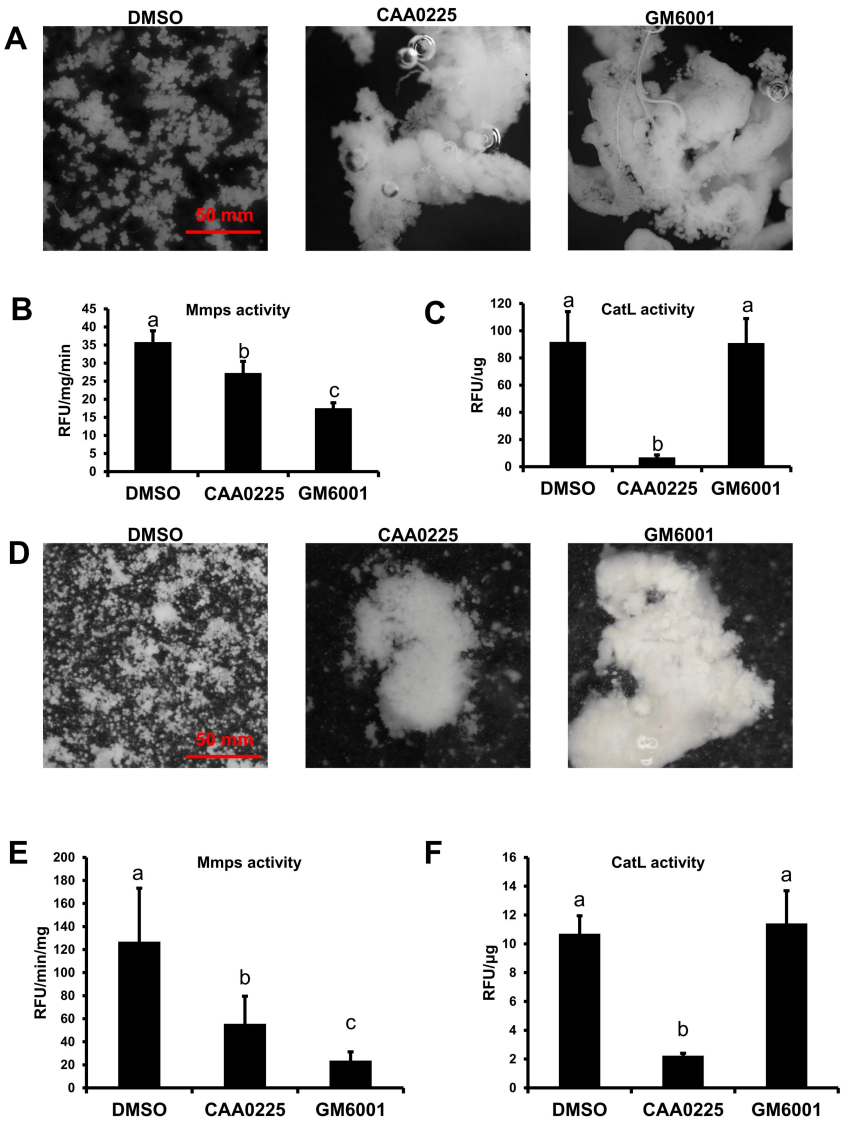

Fig. S2. Mmps act downstream of CatL in fat body cell dissociation in *B. mori* and *S. frugiperda.*

(*A*-*C*) *B. mori* studies. Fat body cell dissociation is delayed upon injection of the CatL inhibitor CAA0225 or the Mmps inhibitor GM6001 (*A*). Fat body Mmps activity is reduced upon injection of CAA0225 or GM6001 (*B*). Fat body CatL activity is reduced upon injection of CAA0225 but is not affected upon injection of GM6001 (*C*).

(*D*-*F*) *S. frugiperda* studies. Fat body cell dissociation is delayed upon injection of CAA0225 or GM6001 (*D*). Fat body Mmps activity is reduced upon injection of CAA0225 or GM6001 (*E*). Fat body CatL activity is reduced upon injection of CAA0225 but is not affected by an injection of GM6001 (*F*).

Bars represent the mean ± SEM. Significant differences were calculated using Student's t test (*, $p<0.05$; **, $p<0.01$) according to three biological replicates.

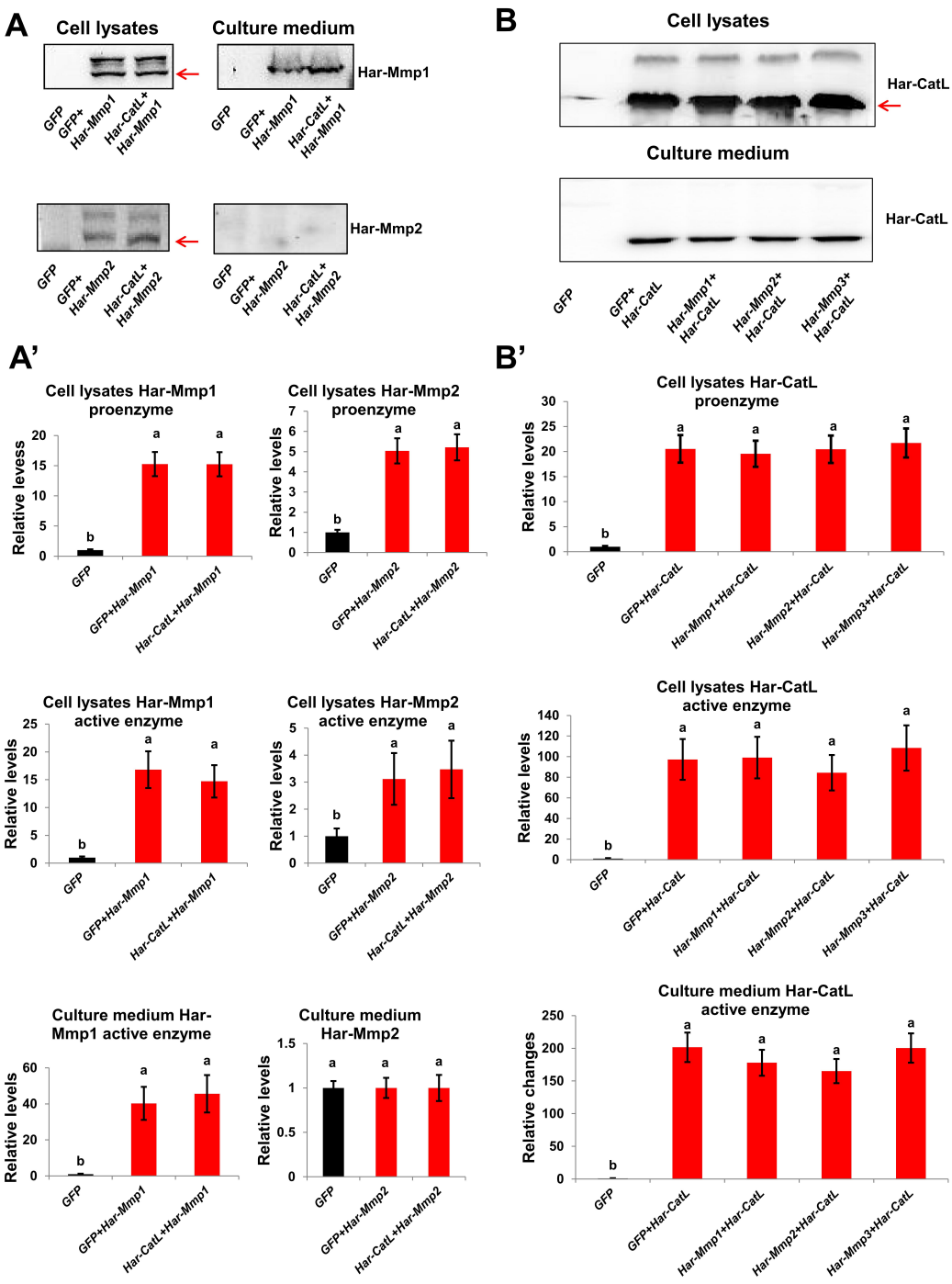

Fig. S3. Analysis of protein-protein interactions between Har-CatL and Har-Mmps.

(*A-A'*) Western blots analysis of the precursor and mature forms of Har-Mmp1 and Har-Mmp2 with *Har-Mmp1* and *Har-CatL*, *Har-Mmp2* and *Har-CatL* co-overexpression in HaEpi cells.

(B-B') Western blots analysis of the precursor and mature forms of Har-CatL with *Har-CatL* and *Har-Mmps* co-overexpression in HaEpi cells.

Bars represent the mean ± SEM. Significant differences were calculated using ANOVA (bars labeled with different lowercase letters are $p<0.05$) according to three biological replicates.

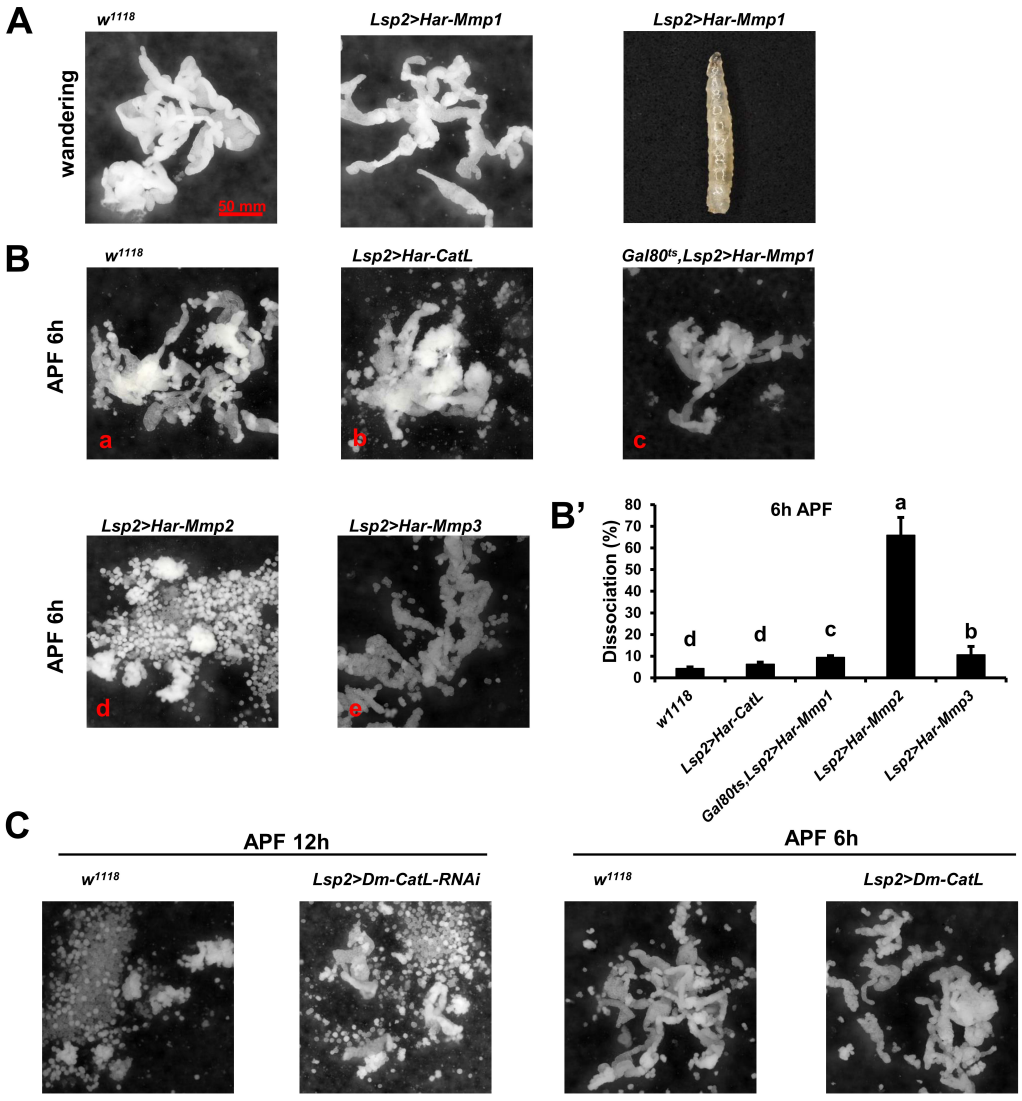

Fig. S4. Overexpression of *Har-Mmp*s, but not *Har-CatL*, induces precocious fat body cell dissociation in *D. melanogaster*.

(*A*) Overexpression of *Har-Mmp1* caused lethality in third instar larvae, but the fat body remained intact.

(*B*) Effects of overexpression of *Har-CatL* and *Har-Mmps* on fat body cell dissociation. Overexpression of *Har-CatL* did not have an obvious effect on fat body cell dissociation (*B-b*). By adding a temperature-sensitive form of the Gal80^{ts} repressor, we overexpressed *Har-Mmp1* 0h after puparium formation (APF), and the fat body cell dissociation was precociously happened at 6h APF (*B-c*). Overexpression of *Har-Mmp2* dramatically induced precocious fat body cell dissociation at 6h APF (*B-d*,), and overexpression of *Har-Mmp3* also caused precocious fat body cell dissociation (*B-e*,).

(*B'*) The quantitation results of (B).

(C) Knockdown of *Dm-CatL* or overexpression of *Dm-CatL* did not have an obvious effect on fat body cell dissociation.

Bars represent the mean ± SEM. Significant differences were calculated using ANOVA (bars labeled with different lowercase letters are $p<0.05$) according to three biological replicates.

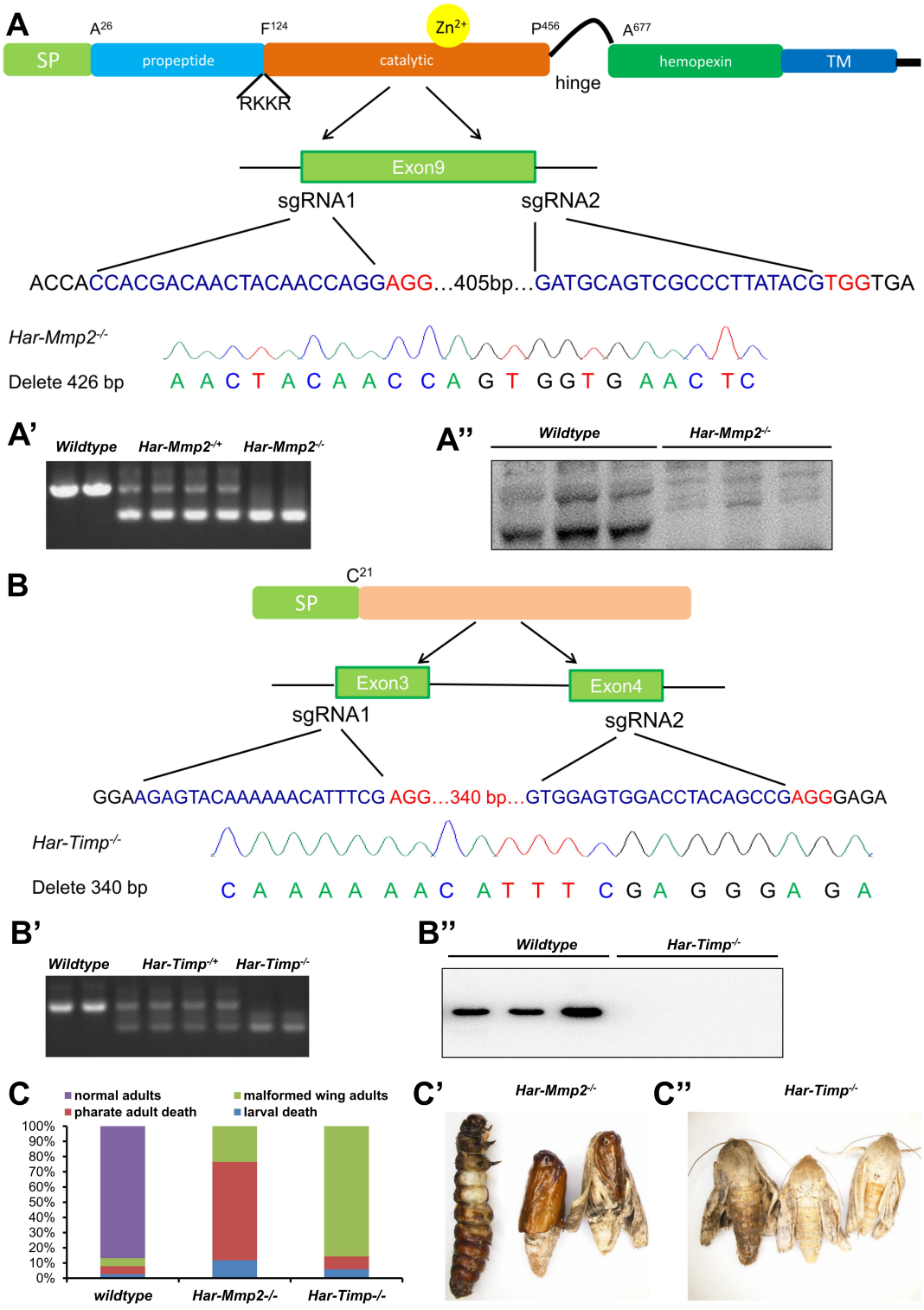

Fig. S5. CRISPR/Cas9-based knockout of *Har-Mmp2* and *Har-Timp*.

(*A-A''*) Generation of the *Har-Mmp2*$^{-/-}$ mutant. Schematic representation showing the Har-Mmp2 protein in *H. armigera*, positions and target sequences of two sgRNAs and a representative chromatogram showing the direct sequencing of PCR products of *Har-Mmp2*$^{-/-}$ mutant individuals (*A*). Genotyping of individual insects and the identification of the *Har-Mmp2*$^{-/-}$ mutant as

determined by the banding patterns of the PCR products (*A'*). Western blots validation of *Har-Mmp2*$^{-/-}$ mutant with anti-DmMmp2 antibody (*A''*).

(*B-B''*) Generation of the *Har-Timp*$^{-/-}$ mutant. Schematic representation showing the Har-Timp protein in *H. armigera*, positions and target sequences of two sgRNAs and a representative chromatogram showing the direct sequencing of PCR products of *Har-Timp*$^{-/-}$ mutant individuals (*B*). Genotyping of individual insects and the identification of the *Har-Timp*$^{-/-}$ mutant on the basis of banding pattern of the PCR products (*B'*). Western blots validation of *Har-Mmp2*$^{-/-}$ mutants using an anti-Har-Timp antibody (*B''*).

(*C-C''*) Phenotypic defects of *Har-Mmp2*$^{-/-}$ mutant and the *Har-Timp*$^{-/-}$ mutant. Statistical analysis of the phenotypes observed in wildtype animals, *Har-Mmp2*$^{-/-}$ mutants and *Har-Timp*$^{-/-}$ mutants (*C*). About 10% *Har-Mmp2*$^{-/-}$ mutants died during larva-pupa transformation, most *Har-Mmp2*$^{-/-}$ mutants survived to the pharate adult stage but failed to emerge as adults (*C'*). *Har-Timp*$^{-/-}$ mutants emerged with twisted wings and died within 3 days (*C''*).

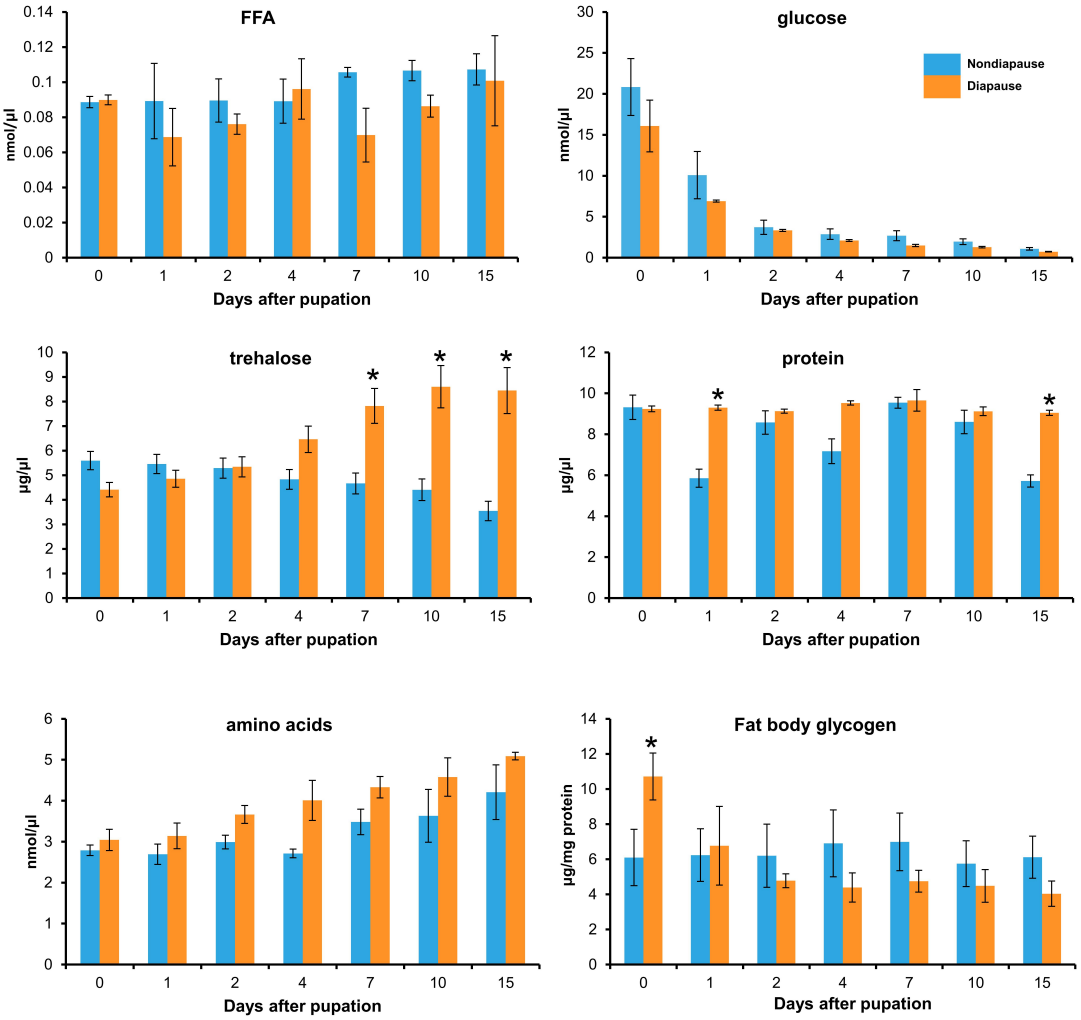

Fig. S6. The developmental patterns of hemolymph FFA, glucose, trehalose, protein, amino acids and fat body glycogen content in nondiapause and diapause pupae.

Bars represent the mean ± SEM. Significant differences were calculated using Student's t test (*, $p<0.05$) according to three biological replicates.

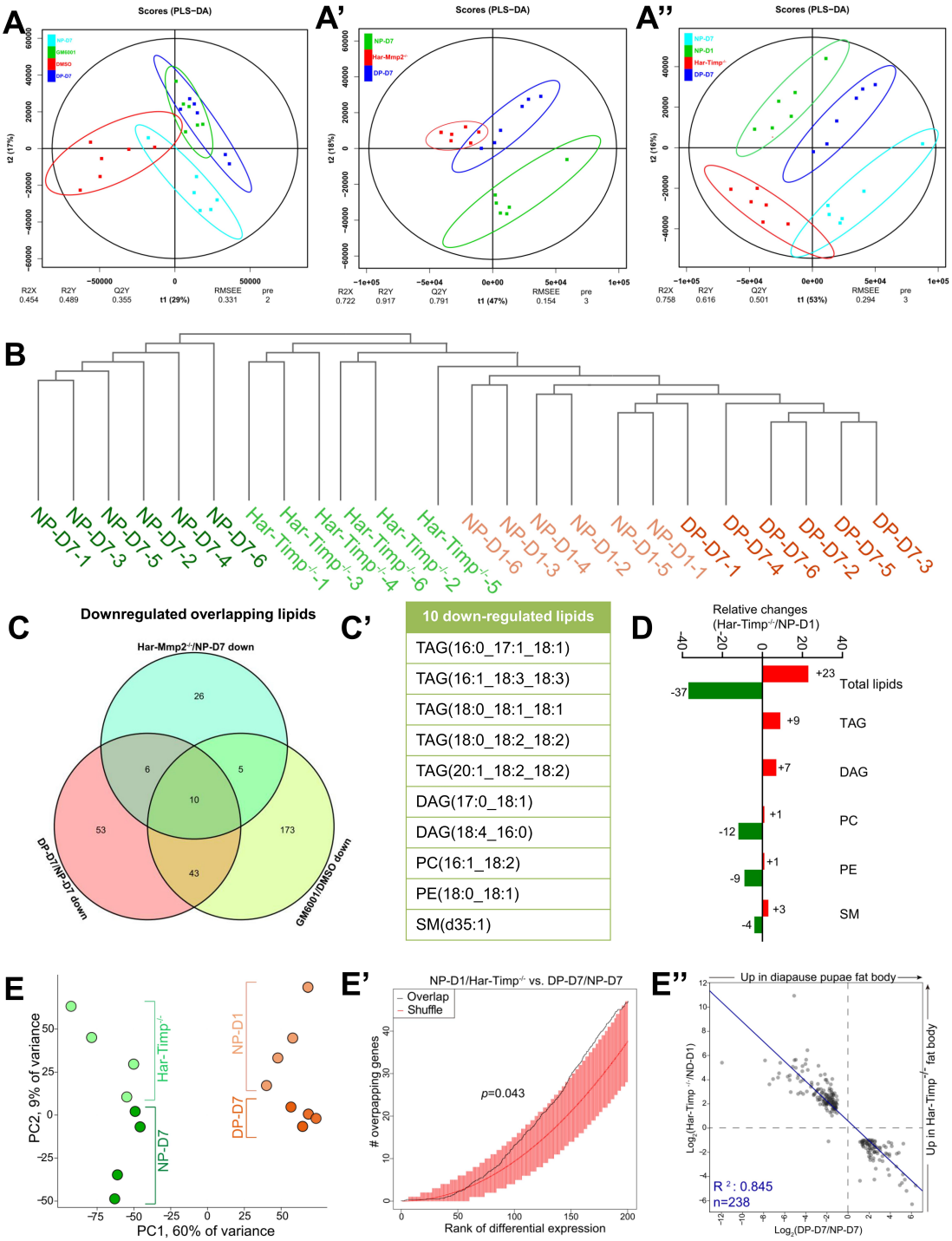

Fig. S7. Lipidomic and transcriptomic analyses of fat body cell dissociation on hemolymph lipid species.

(*A-A''*) PLS-DA plots and scores of DP-D7 vs. NP-D7 vs. DMSO vs. GM6001 (*A*), DP-D7 vs. NP-D7 vs. Har-Mmp2$^{-/-}$ (*A'*) and DP-D7 vs. NP-D7 vs. NP-D1 vs Har-Timp$^{-/-}$ (*A''*).

(*B*) Unsupervised cluster analysis of samples based on the abundance of 621 lipid species profiled in hemolymph isolated from DP-D7, NP-D7, NP-D1 and *Har-Timp*$^{-/-}$ mutant pupae.

(*C-C'*) Venn diagram showing common lipid species with reduced levels upon inhibition of fat body cell dissociation (*C*). Ten common lipid species with reduced levels were found upon inhibition of fat body cell dissociation (*C'*).

(*D*) Changes in total lipid species and various lipid groups differentially expressed following the promotion of fat body cell dissociation.

(*E-E''*) Mutation of *Har-Timp* caused pupal fat body gene expression on day1 shifted toward a day 7 nondiapause-like state. PCA based on the 500 most variable genes showing nondiapause pupae (day 1 and day 7) and diapause pupae and *Har-Timp* $^{-/-}$ pupae (day 1) under nondiapause conditions (*E*). Overlap of genes affected by *Har-Timp* mutation with those differentially expressed in day 7 diapause and non-diapause pupae (black line) (*E'*). Comparison of $\log_2$-fold-change for DEGs present in both the diapause pupae versus nondiapause pupae (day 7) comparison (x axis) and the *Har-Timp*$^{-/-}$ pupae versus nondiapause pupae (day 1) (y axis) (*E''*).

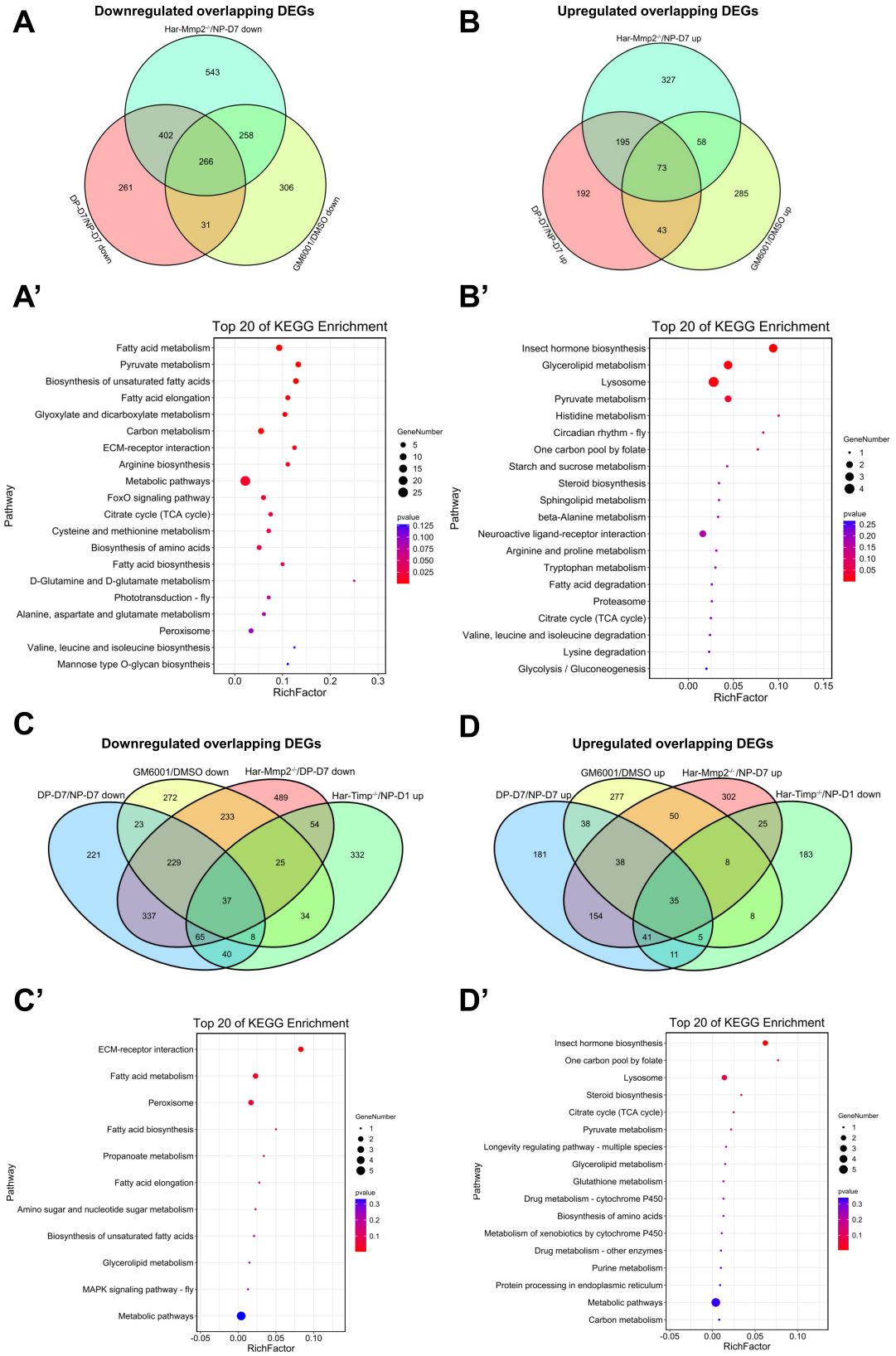

Fig. S8. Overview of the significant enriched pathways in transcriptomic analyses for inhibition or promotion of fat body cell dissociation.

(A-B') The downregulated and upregulated genes upon inhibition of fat body cell dissociation. 266 genes were co-downregulated upon fat body cell dissociation is inhibited as shown in Venn diagram (*A*). The significant enriched pathways of these 266 genes were shown in KEGG pathway enrichment analysis (*A'*); 73 genes were co-upregulated upon fat body cell dissociation is inhibited as shown in Venn diagram (*B*). The significant enriched pathways of these 73 genes were shown in KEGG pathway enrichment analysis (*B'*).

(C-D') The downregulated and upregulated genes upon manipulation of fat body cell dissociation. After overlapping with upregulated genes in the Har-Timp$^{-/-}$/NP-D1 group, 37 genes were co-downregulated upon fat body cells were not dissociated (*C*). The significant enriched pathways of these 37 genes were shown in KEGG pathway enrichment analysis (*C'*); After overlapping with downregulated genes in the Har-Timp$^{-/-}$/NP-D1 group, 35 genes were co-upregulated upon fat body cells were not dissociated (*D*). The significant enriched pathways of these 37 genes were shown in KEGG pathway enrichment analysis (*D'*).

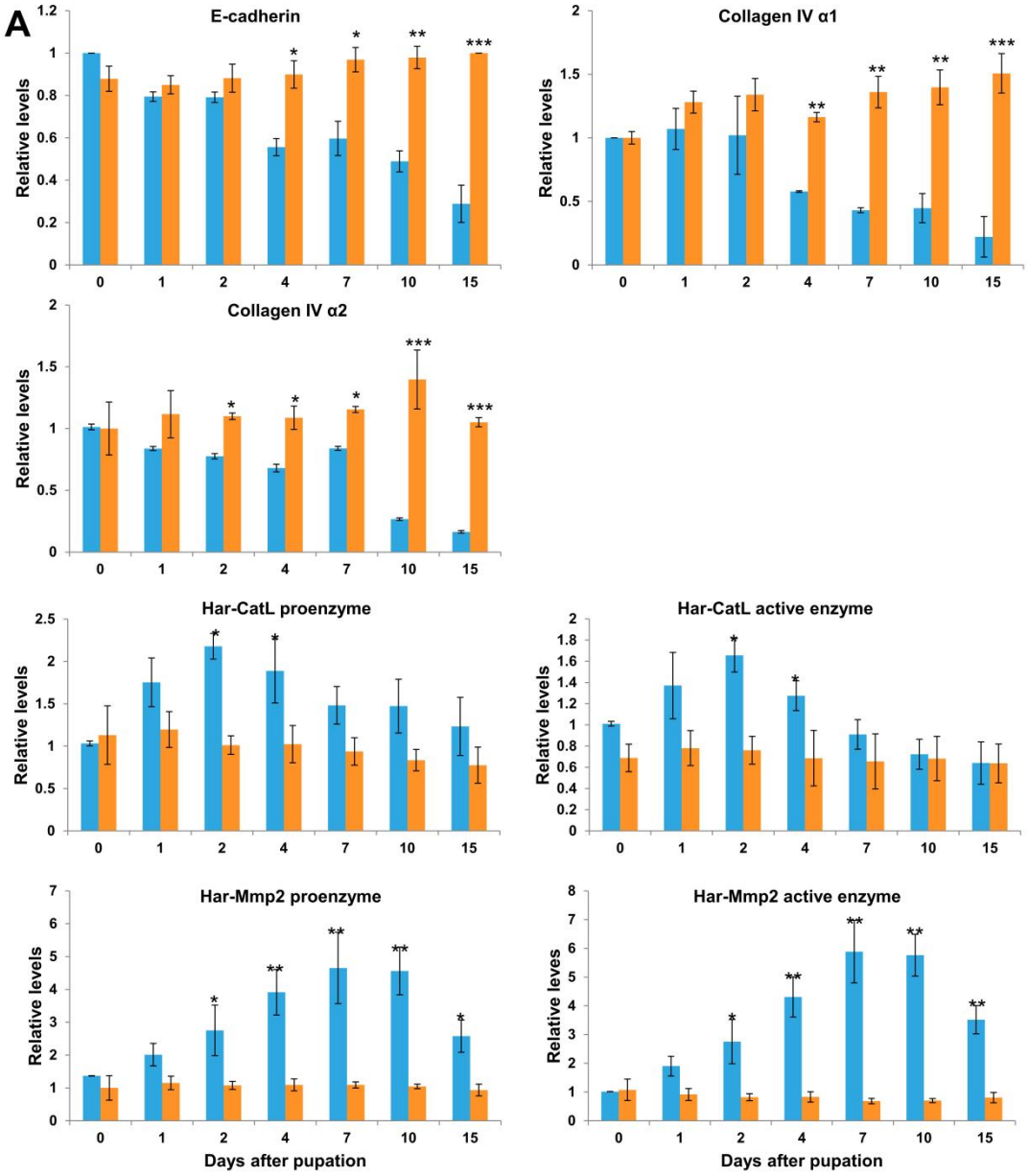
A
E-cadherin
Collagen IV α1
Collagen IV α2
Har-CatL proenzyme
Har-CatL active enzyme
Har-Mmp2 proenzyme
Har-Mmp2 active enzyme
Relative levels
Relative leves
Days after pupation
B
cell lysates
culture medium
cell lysates
culture medium
degraded/intact
active/precursor
relative active form
GFP+Har-Timp
Har-CatL+Har-Timp
Har-CatL+Har-Mmp3
C
E-cadherin
collagen IVα1
collagenIV α2
Relative levels
DMSO
CAA0225
GM6001
wildtype NP-D7
Har-Mmp2-/- NP-D7
Har-Mmp2-/- NP-D14
wildtype NP-D1
Har-Timp-/- NP-D1
rHar-Mmp2 NP-D1

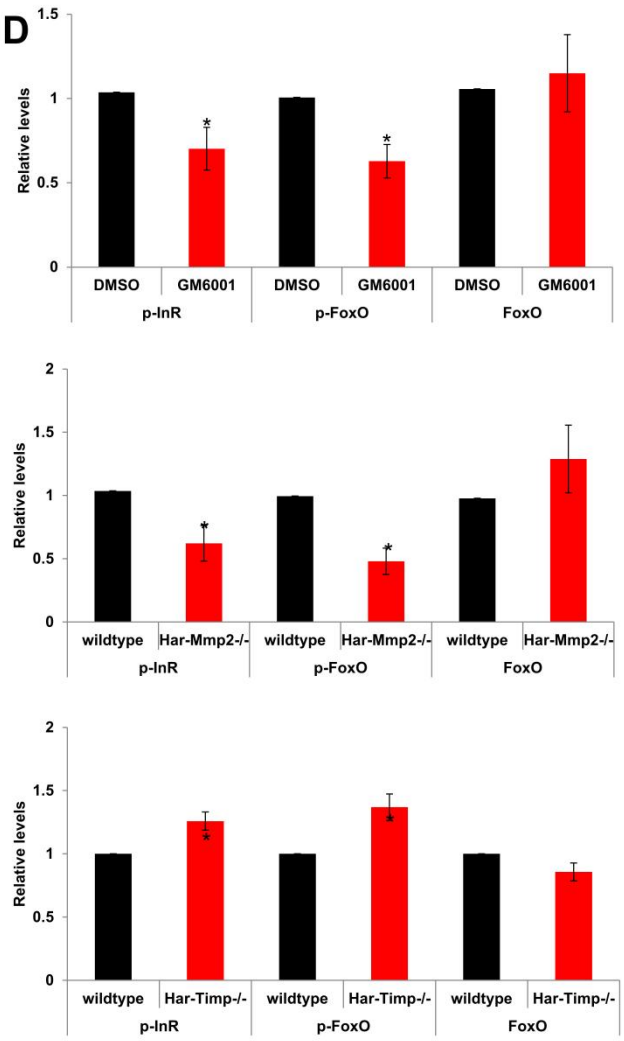

Fig. S9. Quantifications of western blot with IMAGE J.

(A) Relative changes of protein abundance in fat body of diapause and nondiapause pupae, related to Fig. 1B and 1D.

(B) Relative changes of protein abundance in Fig. 2D

(C) Relative changes of protein abundance in Fig. 2A', F' and G'.

(D) Relative changes of protein abundance in Fig. 3E.

Western blot bands from three independent replicates were quantified using IMAGE J software (NIH, Bethesda, MD, USA) and normalized to tubulin levels (A, C, D) or control (B).

Bars represent the mean ± SEM. Significant differences were calculated using Student's t test (*, $p<0.05$; **, $p<0.01$) according to three biological replicates.

Table S1. PCR primers used in this study.

primers for qPCR		
gene	Forward primer	Reverse primer
Rpl32	CCCGTCACATGCTACCCAATGG	CTCGCTCCACGATGGTCTTGC
Har-CatL	AGGGTGACGAGGAGAAGCTGATGC	ACGCCGTCGGAGTAGAACTGGAAG
Har-Mmp1	TACGGTCACAAGACGCAAACAGA	GCCAGTAATGCTCGCCTTTGAATA
Har-Mmp2	ACTGTTTGCCGTGGCTGCTC	AAGTTTGGTTGAATGCCTTGGTA
Har-Mmp3	CGCTACGATGAGAACACGAACA	AGAGCAGCATTCACAGGATAAGG
PCR primers for dsRNA		
GFP	TAATACGACTCACTATAGGATGGT GAGCAAGGGCGAGGAG	TAATACGACTCACTATAGGTTACT TGTACAGCTCGTCCAT
Har-CatL	TAATACGACTCACTATAGG CTGGTTGGGATCGAAGGACA	TAATACGACTCACTATAGG GGTTGCTCAAAGCCATCAGTT
PCR primers for sgRNA		
Har-Mmp2 SgRNA1-FP	GAAATTAATACGACTCACTATAGCCACGACAACTACAACCAGGGTTTTA GAGCTAGAAATAGCAAG	
Har-Mmp2 SgRNA2-FP	GAAATTAATACGACTCACTATAGATGCAGTTGCCCTTATACGGTTTTAGA GCTAGAAATAGCAAG	
Har-Timp SgRNA1-FP	GAAATTAATACGACTCACTATAGAGAGTACAAAAAACATTTCGGTTTTA GAGCTAGAAATAGCAAG	
Har-Timp SgRNA2-FP	GAAATTAATACGACTCACTATAGTGGAGTGGACCTACAGCCGGTTTTAG AGCTAGAAATAGCAAG	
Common sgRNA-RP	AAAAGCACCGACTCGGTGCCACTTTTTCAAGTTGATAACGGACTAGCC TTATTTTAACTTGCTATTTCTAGCTCTAAAAC	

Datasets S1 and S2 (Separate files)

Dataset S1: Differential lipids in the *H.armigera* hemolymph.

Dataset S2: DEGs in the *H.armigera* fat body.